Eur. Phys. J. D **5**, 433–440 (1999)

THE EUROPEAN PHYSICAL JOURNAL D

EDP Sciences

A Fourier optics model of two-beam scanning laser interferometers

A. Bergamin, G. Cavagnero, L. Cordiali, and G. Mana[a]

CNR, Istituto di Metrologia "G. Colonnetti", strada delle Cacce 73, 10135 Torino, Italy

Received: 18 February 1998 / Revised: 21 October 1998 / Accepted: 16 November 1998

Abstract. The article illustrates the use of Fourier optics to describe the operation of two-beam scanning laser interferometers. It deals with the effect of diffraction on the spatial periodicity of a monochromatic and coherent beam. Particular attention is given to the analysis of systematic errors in high-accuracy laser metrology. The article reviews the special case of plane wave and Gaussian illuminations, examines how beam truncation affects the period of traveling fringes and presents a general relation between the relative wavelength deviation and the impulse standard deviation of the photons.

PACS. 42.25.Fx Diffraction and scattering – 42.25.Hz Interference

1 Introduction

Since the late sixties, optical interferometry has been increasingly applied in high-precision measurements, its use having been triggered by the development of lasers and, subsequently, by laser stabilization. However, stabilization alone is not enough to meet the requirements of today's most accurate measurements, such as those necessary in high-resolution spectroscopy in which accurate observations require absolute interferometric measurements of wavelengths to be made to within the 10^{-10} uncertainty level [1]. Another example is the determination of the Avogadro constant [2]. Several laboratories are engaged in reducing the relative uncertainty to the 10^{-8} level, which requires, among other things, laser interferometric measurements to be made to within 10^{-9} relative uncertainty. At these levels of uncertainty, the relation $\lambda = c/\nu$ (the symbols having the usual meanings) is valid only for an ideal plane wave. In reality, some energy disperses outside the region in which it would be expected to remain in plane wave propagation. This effect is known as diffraction and is an important and unavoidable phenomenon connected with the wave nature of light. As a result of diffraction, wavefronts bend and their spacing varies from one point to an other and is different from the wavelength of a plane wave.

Diffraction has been extensively investigated theoretically and experimentally [3–10]. A twofold motivation encouraged us to study this subject further. Firstly, we are engaged in the measurement of the silicon lattice parameter (a basic ingredient in the determination of the Avogadro constant) by combined X-ray and optical interferometry. We have studied diffraction by using the Gaussian approximation of laser beams [7] and subsequently we extended the analysis to beam shear [8] and astigmatism [9]. However, recent improvements led us to increase measurement resolution by one order of magnitude and to consider the matter from an entirely different viewpoint [11]. The potential 10^{-9} accuracy raises questions about correction calculation and about the assessment of how close a beam is to the perfection represented, conceptually, as a Gauss function. Secondly, we considered it useful to exploit Fourier optics as much as possible, since it provides the basis for an elegant formalism, shared with quantum mechanics, which is suitable to describe interferometer operation and to calculate diffraction correction, no matter how complex the illuminating wave may be. Fourier optics can be applied also to study other interferometers; examples are atom and X-ray interferometry [12–14]. In our article, we present, firstly, a formal theory of two-beam scanning interferometry without putting any restricting assumptions on the illuminating beam. Subsequently, we analyze the effect of diffraction, with emphasis on the phase of traveling fringes. Finally, we give a few examples of the calculation of excess-phase and correction.

2 Basic theory

2.1 Impulse representation

In a two-beam interferometer, a laser beam is split into two beams which recombine after propagating in the interferometer arms. To simplify matters, let us consider a two-dimensional interferometer illuminated by a monochromatic wave $E_i(x) = E(x; z = 0)$ which produces two interfering beams $E_1(x; z)$ and $E_2(x; z)$. From a formal point of view, an interferometer can be examined in terms

[a] e-mail: g.mana@imgc.to.cnr.it

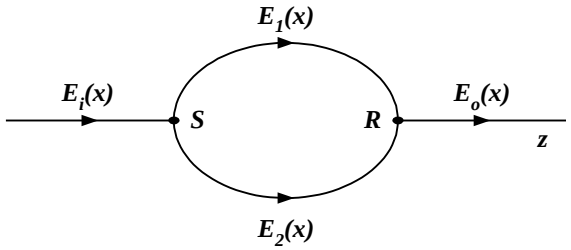

Fig. 1. Schematics of a two-beam interferometer. The incoming beam is split in S, delivered along paths 1 and 2, and recombined in R.

of input-output relations as the transformation of the wave $E_i(x)$ into the wave $E_0(x) = E_1(x) + E_2(x)$, as shown in Figure 1. In order to study diffraction, it is convenient to use the mixed Fourier components of the incoming wave with respect to the x variable [15]

$$\tilde{E}(p;z) = \langle p|E(z)\rangle = \int_{-\infty}^{+\infty} E(x;z)\exp(-\mathrm{i}px)dx. \quad (1)$$

The optical path z is here an evolution parameter, which is selected as a fictitious time. With the use of the mathematical formalism of quantum mechanics, $E(x;z)$ and $\tilde{E}(p;z)$ are the space- and the impulse-domain representations of the abstract state vector $|E(z)\rangle$, which belongs to the space of single-value square-integrable functions. Accordingly, p equals the propagation vector of a plane wave representing free particles of impulse $\hbar p$ in a one-dimensional space. Since the plane wave

$$E(x;z) = \exp(\mathrm{i}\mathbf{k}\cdot\mathbf{r}) = \langle x|p\rangle \quad (2)$$

propagating with wave vector $\mathbf{k} = p\mathbf{e}_x + q\mathbf{e}_z$, where $|\mathbf{k}| = k = 2\pi/\lambda$, is the space-domain representation of the base vector $|p\rangle$, the impulse-domain representation (1) is known as the angular spectrum of $E(x;z)$. Putting γ to indicate the propagation angle of (2) and assuming that $|p| \ll k$, we can write the approximate relation $\gamma = p/k$, which expresses the link between the impulse of the base vector $|p\rangle$ and the direction of the corresponding plane wave.

With the use of impulse-domain representation and the omission of common factors, the waves which leave the interferometer after crossing it along paths 1 and 2 are

$$\tilde{E}_1(p) = \tilde{E}_i(p), \quad (3)$$
$$\tilde{E}_2(p) = U(p;s)\tilde{E}_i(p), \quad (4)$$

where s is the difference between the lengths of the optical paths through the two interferometer arms and

$$U(p;s) = \exp(\mathrm{i}qs), \quad (5)$$

where $q^2 = k^2 - p^2$, is the impulse-domain representation of the free propagator for the wave equation. If $\tilde{E}_i(p)$ does not contain "high frequency" components, which means that $|\tilde{E}_i(p)|^2 \neq 0$ only if $|p| \ll k$, we can use the Fresnel approximation

$$U(p;s) \approx \exp\left[\mathrm{i}k\left(1 - \frac{p^2}{2k^2}\right)s\right]. \quad (6)$$

Consequently,

$$\tilde{E}_2(p) = \exp\left[\mathrm{i}k\left(1 - \frac{p^2}{2k^2}\right)s\right]\tilde{E}_i(p). \quad (7)$$

The detected signal is the integral of the interference pattern

$$S(x) = |E_1(x) + E_2(x)|^2 \quad (8)$$

over the detector aperture. For the sake of simplicity, and since we confine ourselves to the case of limited transverse extension of $E(x;z)$ and of a large detector aperture, we set the integration limits at infinity. According to Parseval's theorem,

$$I = \int_{-\infty}^{+\infty} S(x)dx = \int_{-\infty}^{+\infty} S(p)dp, \quad (9)$$

where

$$S(p) = |\tilde{E}_1(p) + \tilde{E}_2(p)|^2 = |\tilde{E}_i(p)|^2\left|1 + \exp\left[\mathrm{i}ks\left(1 - \frac{p^2}{2k^2}\right)\right]\right|^2. \quad (10)$$

During mirror movements the outgoing beam is intensity modulated. If a plane wave is assumed to propagate through the interferometer, a simple ray tracing shows that the optical-path difference changes by $s\cos\gamma \approx s(1-\gamma^2/2)$, with the propagation angle γ denoting the deviation from the optical axis. Since $\gamma = p/k$, the excess phase in (10) accounts for the cosine error. If we put the mean intensity

$$G = \int_{-\infty}^{+\infty} |\tilde{E}_i(p)|^2 dp, \quad (11a)$$

visibility $\Gamma(s) = |\Xi(s)|/G$, where

$$\Xi(s) = \int_{-\infty}^{+\infty} |\tilde{E}_i(p)|^2 \exp\left(\frac{\mathrm{i}sp^2}{2k}\right)dp, \quad (11b)$$

and excess phase $\Phi(s) = \arg[\Xi(s)]$, we can write (9) in the form

$$I(s) = 2G\{1 + \Gamma(s)\cos[ks - \Phi(s)]\}. \quad (11c)$$

The use of the Fresnel approximation corresponds to approximating the wave equation by means of the Schrödinger-type equation

$$\mathrm{i}\partial_z|E(z)\rangle = H|E(z)\rangle, \quad (12)$$

where $H = p^2/2k$. Therefore, by solving the Heisenberg-type equation of motion

$$\mathrm{i}\partial_z\sigma_x^2(z) = \langle E(z)|[x^2, H]|E(z)\rangle, \quad (13)$$

which gives the evolution of the position variance of photons

$$\sigma_x^2(z) = \langle E(z)|x^2|E(z)\rangle = \frac{\int_{-\infty}^{+\infty} x^2|E(x;z)|^2dx}{\int_{-\infty}^{+\infty}|E(x;z)|^2dx}, \quad (14)$$

one can prove that, with a suitable choice of the origin, $\sigma_x^2(z)$ obeys the free space propagation rule [16]

$$\sigma_x^2(z) = \sigma_0^2 + \frac{\sigma_p^2}{k^2}z^2, \quad (15)$$

where $\sigma_x^2 = \sigma_0^2(z=0)$ is the position variance of photons at the "initial time" and

$$\sigma_p^2 = \langle E(z)|p^2|E(z)\rangle = \frac{\int_{-\infty}^{+\infty} p^2|\tilde{E}(p;z)|^2dp}{\int_{-\infty}^{+\infty}|\tilde{E}(p;z)|^2dp}, \quad (16)$$

is the impulse variance of photons. It must be noted that, owing to the fact that the impulse is a constant of motion, free propagation does not change $\tilde{E}(p;z)$. Therefore, beam amplitude and intensity profile change with propagation, but $|\tilde{E}(p)|^2$ does not and the impulse variance σ_p^2 is constant. Physically, if the wave encounters no obstacles, the impulse distribution does not change. For any arbitrary beam, the position variance reaches its minimum σ_0^2 at a certain waist point and varies quadratically with z on either side of that point. By defining, from analogy with the Gaussian case, the spot size $w(z) = 2\sigma_x(z)$, the formula (15) is like that expressing the free-space variation of the spot size of a Gaussian beam. Hence the divergence angle

$$\theta = 2\sigma_p/k, \quad (17)$$

can unambiguously be defined for any real beam. Since x and p are conjugate variables and $\sigma_0 < \sigma_x(z)$, the Heisenberg uncertainty principle,

$$2\sigma_p\sigma_0 = M^2 \geq 1, \quad (18)$$

which, by using (17) and $w_0 = 2\sigma_0$, can be also written $\theta w_0 \geq 2/k$, states that there is a minimum possible product of spot size and divergence. As the waist size is squeezed down, the uncertainty in photon localization is improved, but the uncertainty in impulse increases and the beam diverges as it propagates. The uncertainty product provides a means for a definition of photon localization and of beam quality [17,18]: the dimensionless propagation parameter M^2 defined in (18) measures the beam spread and $M^2 = 1$ corresponds to a diffraction-limited beam.

If we put $u = \sigma_0 p$ to indicate the impulse of the plane wave components of $|E_i\rangle$, the tangent of the excess phase is

$$\tan\Phi(s) = \frac{\int_{-\infty}^{+\infty}|\tilde{E}_i(u)|^2\sin(2\xi u^2)du}{\int_{-\infty}^{+\infty}|\tilde{E}_i(u)|^2\cos(2\xi u^2)du}, \quad (19)$$

where $\xi = s/(4z_R)$ and $z_R = k\sigma_0^2$ is the Rayleigh range. The use of the dimensionless impulse u and optical path difference ξ allows different physical situations to be described by the same equations and brings into light their common scale and underlying equivalence.

2.2 Correction for diffraction

According to (11c), mirror movements give rise to traveling fringes. Diffraction causes distortion of fringes, and makes their period

$$\lambda_{eff} = \lambda\left(1 + \frac{1}{k}\frac{d\Phi}{ds}\right) \quad (20)$$

different from that obtained when the illuminating wave is plane. The corrective term for the period of traveling fringes is

$$\frac{\Delta\lambda}{\lambda} = \frac{1}{k}\frac{d\Phi}{ds} = \frac{\theta^2}{4}\left(\frac{1}{M^2}\frac{d\Phi}{d\xi}\right), \quad (21)$$

where the term enclosed within parentheses gives the "invariant" part of the correction and the factor the scale. The asymptotic behaviour of the excess phase when the optical-path difference tends to infinity can be obtained by application of the stationary-phase method. Thus,

$$\lim_{s\to\infty}\Phi(s) = \pi/4. \quad (22)$$

With the optical-path difference tending to zero, the excess phase is

$$\lim_{s\to 0}\Phi(s) = \frac{s\sigma_p^2}{2k}, \quad (23)$$

and the correction for diffraction

$$\frac{\Delta\lambda}{\lambda}\Big|_{s\to 0} = \frac{\sigma_p^2}{2k^2}, \quad (24)$$

is proportional to the width of the impulse-domain representation of $|E_i\rangle$. Equation (24) is a central result. It expresses the relative deviation of the $E_i(x;z)$ wavelength with respect to a plane wave in terms of the impulse standard deviation of photons and reduces its computation to the computation of the beam power spectrum, which can be performed by using the Fourier transforming properties of converging lenses. It should be noted that, since free propagation does not change $|\tilde{E}_i(p)|^2$, the time z at which the Fourier transform operation is performed is not

a cause for concern and that (15) gives the basis for making σ_p measurements also by means of a least squares fit of the beam widths σ_x *versus* distance z. Equation (24) can be simply interpreted as the mean cosine error of the plane wave components of $|E_i\rangle$. In fact, by assuming the beam axis to be parallel to the interferometer optical axis and plane waves to be represented by rays, (24) is the weighted mean of the cosine error for each ray, the weight being the ray intensity $|E_i(\gamma)|^2$ and misalignment being the ray angle $\gamma = p/k$.

For any arbitrary beam, we can express the diffraction correction in terms of divergence, which is easy to measure and rigorously defined for any given beam. Hence,

$$\frac{\Delta\lambda}{\lambda}\Big|_{s\to 0} = \frac{1}{8}\theta^2 \tag{25a}$$

and the inequality

$$\frac{\Delta\lambda}{\lambda}\Big|_{s\to 0} \geq \frac{1}{2k^2 w_0^2} \tag{25b}$$

is valid. In the specific case of Gaussian illumination, diffraction correction has already been obtained and reported by several authors [4–7]. Only in this case does the product of waist size by divergence take the minimum value and equations (25a, 25b) are equivalent; if the illumination is not Gaussian, the equality sign in (25b) is not valid. A second key result is that, since we have not used the explicit form of $E_i(x)$ in obtaining (24) and (25a), our results are valid no matter what the actual illumination may be. To our knowledge, the validity of (25a) for any kind of coherent illumination has so far never been suspected.

We now establish more precisely the assumptions underlying the Fresnel approximation and the meaning of $s \to 0$ in (24). If $\sigma_p \ll k$, the assumption that $\tilde{E}_i(p)$ does not contain high-frequency components is correct. Then, from the uncertainty principle, we obtain $\sigma_0 \gg \lambda$. Consequently, we can use the Fresnel approximation whenever the spot size at the beam waist is much greater than the wavelength. As regards the asymptotic behaviour of the diffraction correction when the optical-path difference is small, in order to obtain (24) the trigonometric functions in (19) must be adequately be approximated by the linear terms of their series expansions. Since $|\tilde{E}_i(p)|^2$ acts as a band-pass filter having bandwidth σ_p, only the $|p| < \sigma_p$ components contribute to the integrals. Consequently, to be accurate, equations (24, 25a) require that the optical-path difference satisfies the inequality $s\sigma_p^2/(2k) \ll 1$, so that, from the uncertainty principle, we obtain $s \ll 4z_R$ or, equivalently, $\xi \ll 1$.

2.3 Three-dimensional case

The formal extension of our results to a three-dimensional interferometer is straightforward. Additionally, if the illuminating wave is separated into two factors, each dependent on only one rectangular coordinate, its impulse-domain representation is the product of two one-dimensional Fourier transforms and calculations simplify into a succession of one-dimensional manipulations. Hence, the impulse variance is defined in terms of rectangular variances as $\sigma_p^2 = \sigma_{px}^2 + \sigma_{py}^2$ and

$$\frac{\Delta\lambda}{\lambda}\Big|_{s\to 0} = \frac{\theta_x^2 + \theta_y^2}{8}\,. \tag{26}$$

Additionally, if $\theta_x = \theta_y = \theta$ diffraction correction is $1/(4\theta^2)$. Another important class of separable functions are those having circular symmetry. By exploiting the transformations into polar coordinates, $r^2 = x^2 + y^2$ and $p^2 = p_x^2 + p_y^2$, in both the xy and $p_x p_y$ spaces, the Fourier transform can be written [15]

$$\tilde{E}(p;z) = 2\pi \int_0^\infty r J_0(rp) E(r;z) dr, \tag{27}$$

where $J_0(rp)$ is the Bessel function of order zero.

3 Examples

We consider now a number of examples of calculations of the excess phase and of the correction for diffraction.

3.1 Gauss function

We consider first the interferometer illuminated by a monochromatic Gaussian beam. In the general case, the beam is astigmatic, but it can always be separated into two factors, each dependent on one rectangular coordinate. Hence, the underlying problem is one-dimensional. To simplify calculations, let us set $z = 0$ at the beam waist, so that

$$E_i(x) = \exp(-x^2/w_0^2) \tag{28}$$

and

$$\tilde{E}_i(u) = w_0\sqrt{\pi}\exp(-u^2), \tag{29}$$

with $u = \sigma_0 p$, $\sigma_0 = w_0/2$ being the variance of (28). By using the dimensionless optical path difference $\xi = s/(4z_R)$, the excess phase of traveling fringes and diffraction correction are

$$\tan\Phi(\xi) = \frac{\sqrt{1+\xi^2}-1}{\xi}, \tag{30}$$

$$\begin{aligned}\frac{\Delta\lambda}{\lambda} &= \frac{\theta^2}{4}\frac{d\Phi}{d\xi} \\ &= \frac{\theta^2}{4}\left(\frac{\sqrt{1+\xi^2}-1}{2\sqrt{1+\xi^2}(1+\xi^2-\sqrt{1+\xi^2})}\right),\end{aligned} \tag{31}$$

respectively. It is well worth calculating the excess phase and its derivative for a circularly symmetric beam. The results are

$$\tan\Phi(\xi) = \xi/2 \tag{32}$$

and

$$\frac{\Delta\lambda}{\lambda} = \frac{\theta^2}{4}\frac{d\Phi}{d\xi} = \frac{\theta^2}{4}\left(\frac{1}{1+\xi^2}\right). \tag{33}$$

3.2 Rectangle function

In the foregoing example, the transverse extent of E_i was infinite. A finite interferometer aperture can be represented by a pupil function which is 1 inside the aperture and is otherwise zero. Let us start by considering a plane wave masked by a rectangular aperture, so that E_i is separated into factors, each dependent on one rectangular coordinate, and the underlying problem is one-dimensional. Then,

$$E_i(x) = \begin{cases} 1 \text{ if } |x| \le a \\ 0 \text{ if } |x| > a \end{cases}, \tag{34}$$

where $2a$ is the aperture side, and

$$\tilde{E}_i(u) = \frac{2a \sin(\sqrt{3}u)}{\sqrt{3}u}, \tag{35}$$

where $u = \sigma_0 p$, with $\sigma_0^2 = a^2/3$ being the variance of (34). Although the excess phase could be written in terms of generalized hypergeometric series, it is better evaluated by numerical quadrature and its derivative by finite differences.

Since the impulse variance σ_p^2 diverges, the analytical approach outlined for the estimate of the diffraction correction in the limit case of a small optical path difference requires further analysis. A weak point is the assumption of an unlimited detector aperture, introduced in order to substitute integration in the impulse domain for integration in the space domain. If one analyses any beam having an infinitely sharp edge, such as the rectangle function, one finds that large-angle and evanescent waves contribute to the interference pattern. To deal effectively with such situations, one should truncate the impulse-domain representation of $|E_i\rangle$. We outline here a procedure for doing this for any beam. Diffraction calculations can be simplified if restrictions more stringent than those used in the Fresnel approximation are adopted. In particular, let us consider free propagation in the space-domain. Hence

$$E(x'; z) = \int_{-\infty}^{+\infty} U(x' - x) E(x; z = 0) dx, \tag{36}$$

where, apart from the phase factor $\exp(-\mathrm{i}\pi/4)$ which will be omitted,

$$\begin{aligned} U(x) &= \frac{1}{2\pi} \int_{-\infty}^{+\infty} U(p) \exp(\mathrm{i}px) dp \\ &= \frac{\exp(\mathrm{i}kz)}{\sqrt{\lambda z}} \exp\left(\frac{\mathrm{i}kx^2}{2z}\right) \end{aligned} \tag{37}$$

is the space-domain representation of the free propagator. If, in addition to $|p| < k$, there are adopted $\langle x \rangle = 0$ and the stronger assumption $2z \gg z_R$, we can use the Fraunhofer approximation

$$\begin{aligned} E(x'; z) = &\frac{\exp\left[\mathrm{i}k\left(1 + \dfrac{kx'^2}{2z}\right)z\right]}{\sqrt{\lambda z}} \\ &\times \int_{-\infty}^{+\infty} E(x; z = 0) \exp(-\mathrm{i}kxx'/z) dx. \end{aligned} \tag{38}$$

Consequently, when z tends to infinity the field amplitude is the Fourier transform of $E(x)$ with a multiplicative factor. The conditions required for the Fraunhofer approximation to be valid are severe, but (38) remains valid if the observation plane is the focal plane of a converging lens, or if the interferometer is illuminated by a wave converging toward the observation plane. For our purposes, the most interesting property of a converging lens is its capability to perform Fourier transformations [15]: the intensity distribution over the focal plane is equal to the power spectrum. To give an example, if the interference pattern is observed in the focal plane of a converging lens, the detector aperture b limits the impulse-domain integrations to $\beta = kb/f$, where f is the lens focal length. More generally, a converging lens maps the different plane wave components of $|E_i\rangle$ into different points of the focal plane and allows specific contributions to the interference pattern to be selected by spatial filtering techniques.

3.3 Truncated Gauss function

We consider now the case when an interferometer has a finite aperture and is illuminated by a Gaussian beam. Let us consider a simple rectangular aperture, so that the underlying problem is one-dimensional, and consider the aperture located at the beam waist. Thus, if $2a$ is the aperture side,

$$E_i(x) = \begin{cases} \exp(-x^2/w_0^2) \text{ if } |x| \le a \\ 0 \qquad\qquad\quad \text{if } |x| > a \end{cases}. \tag{39}$$

The standard deviation of (39)

$$\sigma_0(\alpha) = w_0 \sqrt{\frac{1}{4} - \frac{\alpha \exp(-2\alpha^2)}{\sqrt{2\pi}\,\mathrm{erf}(\sqrt{2}\alpha)}}, \tag{40}$$

where $\alpha = a/w_0$ and erf is the error function, is shown in Figure 2. It is well worth noting that the Gauss and rectangle functions are the limit cases of (39) when α tends to infinity and to zero, respectively. The amplitudes of the plane wave components of (39)

$$\begin{aligned} \tilde{E}_i(p) = &\frac{w_0\sqrt{\pi}}{2} \exp(-w_0^2 p^2/4) \\ &\times \mathrm{erf}(\alpha + \mathrm{i}w_0 p/2) + c.c., \end{aligned} \tag{41}$$

are shown in Figure 3. In the figure, the abscissa is the dimensionless impulse $u = \sigma_0 p$, which allows a comparison of the spectra originated by different interferometer apertures and by the limit cases. The impulse-domain radius of the truncated beam is always greater than that of a Gauss function and diffraction rings are already evident when $\alpha = 1$, that is, when the beam is truncated at the $1/e^2$ radius. When α tends to infinity, the error function tends to one, making (41) a Gauss function, whereas, when α tends to zero, $\tilde{E}_i(u)$ tends to (35).

The excess phase and its derivative are shown in Figures 4 and 5, where different interferometer apertures and

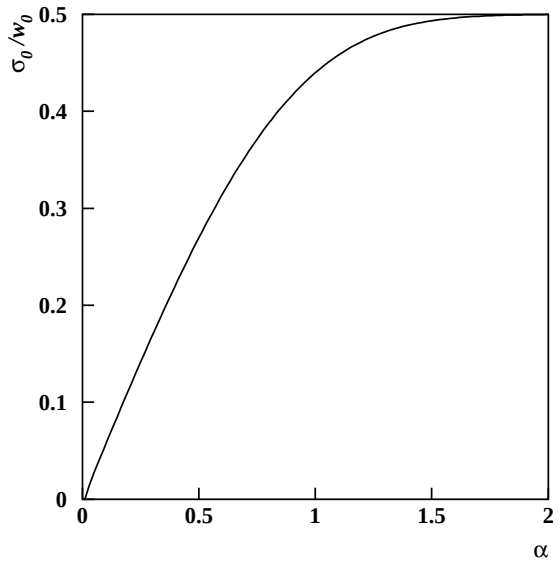

Fig. 2. Standard deviation of a truncated Gauss function *vs.* interferometer aperture $\alpha = a/w_0$.

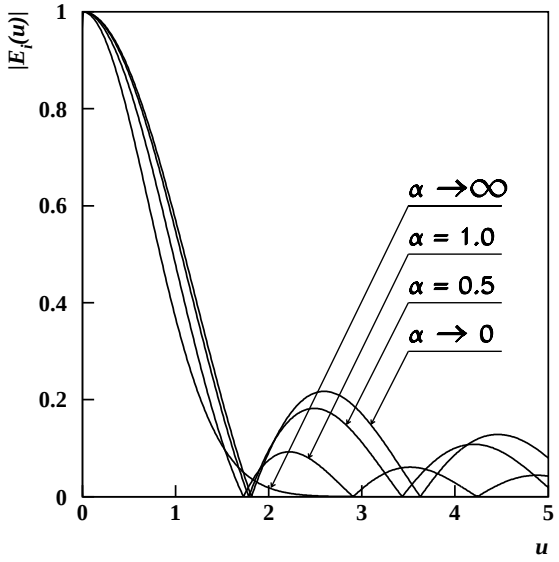

Fig. 3. Amplitude spectrum of a truncated Gauss function *vs.* dimensionless impulse $u = \sigma_0 p$. Different values of interferometer aperture $\alpha = a/w_0$ are considered. The value at the origin is normalized to one. The limit cases $\alpha \to 0$ and $\alpha \to \infty$ correspond to rectangle and Gauss functions, respectively.

the limit cases when the interferometer is illuminated by a Gauss or by a rectangle function are compared. It must be noted that graphs are enclosed between the excess phases which had resulted from a Gauss function and from a rectangle function. We evaluated the excess phase by numerical quadrature of (19) and its derivative by finite differences. Consequently, the only assumptions made in obtaining the curves shown in Figures 4 and 5 are those ensuring that the Fresnel approximation is valid and no restriction is made on the optical path difference. Since the integrands are oscillatory, we integrated between successive zeroes and added the alternating results. As the

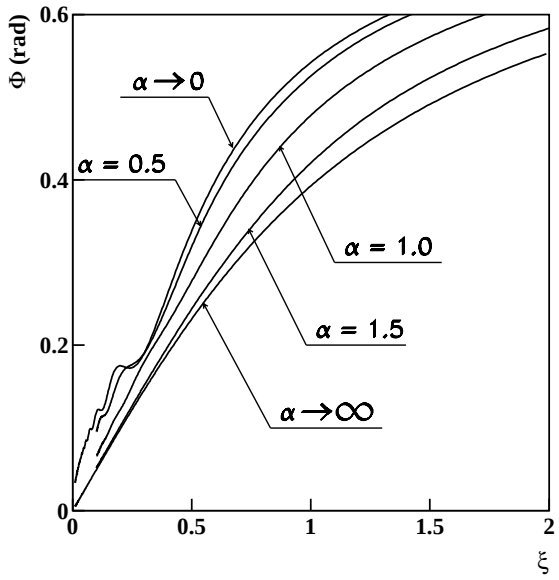

Fig. 4. Excess phase *vs.* dimensionless optical-path difference $\xi = s/(4z_R)$ for a truncated Gauss function. The dimensionless variable $\alpha = a/w_0$ represents the interferometer aperture. The limit cases $\alpha \to \infty$ and $\alpha \to 0$ correspond to Gauss and rectangle functions, respectively.

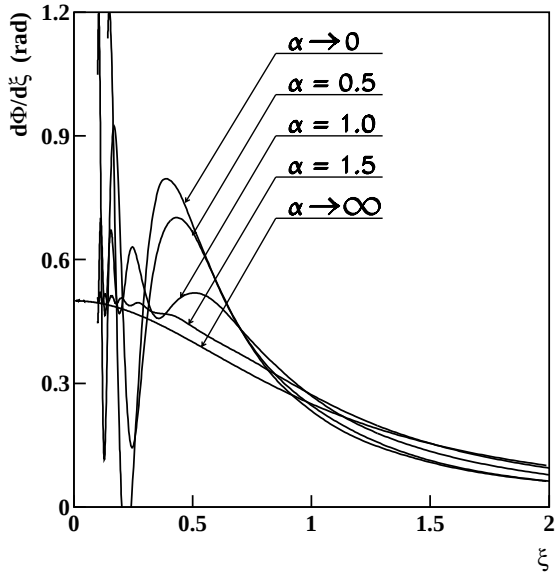

Fig. 5. Derivative of the excess phase *vs.* dimensionless optical-path difference $\xi = s/(4z_R)$ for a truncated Gauss function. The dimensionless variable $\alpha = a/w_0$ represents the interferometer aperture. The limit cases $\alpha \to \infty$ and $\alpha \to 0$ correspond to Gauss and rectangle functions.

optical-path difference ξ tends to zero, the derivative increasingly oscillates and an increasing number of zeroes, even infinite, is required to get a reasonably accurate value of the derivative. For this reason, instabilities prevented us from evaluating the derivative in the neighbourhood of the origin.

As u tends to infinity, $|\tilde{E}_i(u)|^2$ falls off only as $1/u^2$. Therefore, σ_p^2 diverges. In order to estimate diffraction

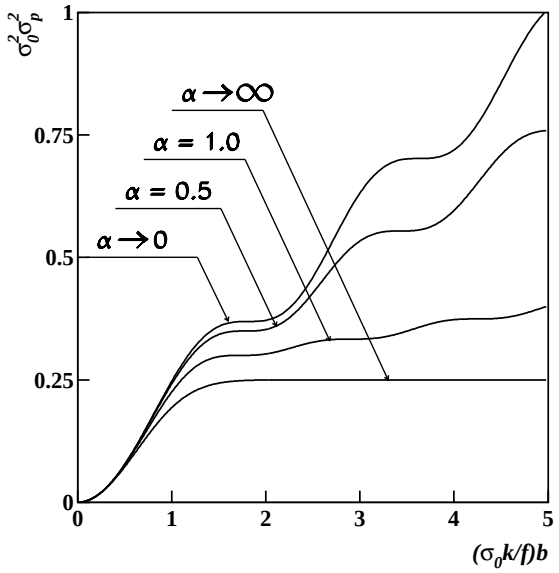

Fig. 6. Impulse variance of a truncated Gauss function *vs.* detector aperture b. Different values of interferometer aperture $\alpha = a/w_0$ are considered. The limit cases $\alpha \to \infty$ and $\alpha \to 0$ correspond to Gauss and rectangle functions, respectively.

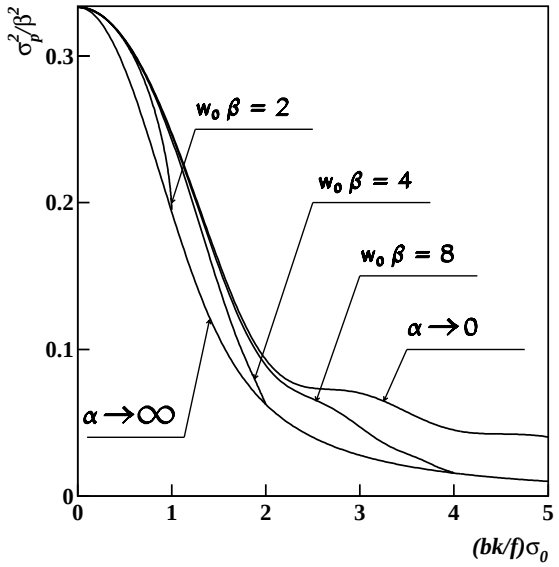

Fig. 7. Impulse variance of a truncated Gauss function *vs.* interferometer aperture σ_0. Different values of detector aperture $\beta = bk/f$ are considered. The limit cases $\alpha \to \infty$ and $\alpha \to 0$ correspond to the impulse variance of a Gauss function *vs.* waist size ($\sigma_0 = w_0/2$) and of a rectangle function *vs.* interferometer aperture ($\sigma_0 = a/3^{1/2}$).

correction, we must take the detector aperture, which, therefore, plays an important role in the interferometer operation, into account. Results are shown in Figures 6 and 7. Figure 6 shows the impulse variance as a function of the detector aperture b with fixed interferometer aperture α,

$$\sigma_0^2\sigma_p^2(b) = \frac{\displaystyle\int_0^{\sigma_0\beta} u^2|\tilde{E}_i(u)|^2\,du}{\displaystyle\int_0^{\sigma_0\beta} |\tilde{E}_i(u)|^2\,du}, \tag{42}$$

where the integration limit is $\sigma_0\beta = kb\sigma_0/f$, $u = \sigma_0 p$, and σ_0 is given by (40). For any given detector aperture, the integration limit can be varied also by changing the interferometer aperture, which is conveniently represented by σ_0. Figure 7 shows, consequently, the impulse variance as a function of σ_0 with the detector aperture, which is conveniently represented by β, fixed,

$$\frac{\sigma_p^2(\sigma_0)}{\beta^2} = \frac{1}{\sigma_0^2\beta^2}\frac{\displaystyle\int_0^{\sigma_0\beta} u^2|\tilde{E}_i(u)|^2du}{\displaystyle\int_0^{\sigma_0\beta} |\tilde{E}_i(u)|^2du}\,. \tag{43}$$

Since diffraction rings cross the detector edge in succession, with the aperture of the detector or of the interferometer increasing, the curves in Figures 6 and 7 oscillate. In the figures, the abscissa, is the integration limit in the u-space, but the independent variable is b in Figure 6 and σ_0 in Figure 7. We made this choice in order to compare different detector and interferometer apertures and the limit cases when the interferometer is illuminated by a Gauss or by a rectangle function. When the detector aperture tends to zero, we select the plane wave propagating along the optical axis and, as Figure 6 shows, diffraction correction is zero. When it is a matter of Gauss and rectangle functions, Figure 7 needs the following additional specifications. Firstly, in the figure, all cases with the same $w_0\beta$ product are described by the same curve. Secondly, when α tends to zero, (39) is a rectangle function, the limit curve is the same for any given value of β, and the abscissa represents the interferometer aperture, $a/\sqrt{3}$. In this case, when a tends to infinity, $|E_i\rangle$ is a plane wave and σ_p^2 is zero, as expected, and, when a tends to zero, $|E_i\rangle$ is a spherical wave and σ_p^2 equals $\beta^2/3$. Thirdly, when α tends to infinity, (39) is a Gauss function, the limit curve is here, too, independent of the β value, and the abscissa represents the waist size $\sigma_0 = w_0/2$. Fourthly, in the remaining cases, the beam begins as a rectangular function and, as σ_0 increases, it becomes a Gauss function. However, the maximum permissible value of σ_0 is $w_0/2$ and the curves end when they join the limit curve corresponding to the Gauss function.

4 Conclusions

This study of diffraction in two-beam interferometers supplements the analysis of the error budget of the silicon lattice parameter value and provides a safer theoretical footing for the study of systematic errors in high-accuracy laser interferometry. It allows the effect of deviations from an ideal Gauss function on measurement accuracy to be

quantified and, additionally, suggests how the relevant correction could be calculated or determined by means of ad hoc experiments. It reveals also that diffraction does not cause errors which cannot be dealt with.

References

1. B. Boldermann, G. Boensch, H. Knoeckel, A. Nicolaus, E. Tiemann, Metrologia **35**, 105 (1998).
2. G. Mana, G. Zosi, Riv. Nuovo Cimento **18**, 1 (1995).
3. W.J. Tango, R.Q. Twiss, Appl. Opt. **13**, 1814 (1974).
4. K. Dorenwendt, G. Bonsch, Metrologia **12**, 57 (1976).
5. J.-P. Monchalin, M.J. Kelly, J.E. Thomas, N.A. Kumit, A. Szoke, F. Zernike, P.H. Lee, A. Javan, Appl. Opt. **20**, 736 (1981).
6. G. Bonsch, Appl. Opt. **22**, 4314 (1983).
7. G. Mana, Metrologia **26**, 87 (1989).
8. A. Bergamin, G. Cavagnero, G. Mana, Phys. Rev. A **49**, 2167 (1994).
9. A. Bergamin, G. Cavagnero, L. Cordiali, G. Mana, IEEE Trans. Instr. Meas. **46**, 196 (1997).
10. R. Masui, Metrologia **34**, 125 (1997).
11. A. Bergamin, G. Cavagnero, L. Cordiali, G. Mana, G. Zosi, IEEE Trans. Instr. Meas. **46**, 576 (1997).
12. M.A.N. Marte, J.I. Cirac, P. Zoller, J. Mod. Opt. **38**, 2265 (1991).
13. G. Mana, E. Vittone, Z. Phys. B **102**, 189 (1997).
14. G. Mana, E. Vittone, Z. Phys. B **102**, 197 (1997).
15. J.W. Goodman, *Introduction to Fourier optics* (Mc. Graw-Hill, New York, 1968).
16. C. Cohen-Tannoudji, B. Diu, F. Laloë, *Quantum Mechanics* (Wiley, New York, 1977).
17. A.E. Siegman, in *Optical Resonators*, SPIE **1224**, 2 (1990).
18. M.W. Sasnett, T.F. Johnston Jr., in *Laser Beam Diagnostic*, SPIE **1414**, 21 (1991).